

A Tree-based Federated Learning Approach for Personalized Treatment Effect Estimation from Heterogeneous Data Sources

Xiaoqing Tan

Department of Biostatistics, University of Pittsburgh, Pittsburgh, PA

and

Chung-Chou H. Chang

Department of Medicine and Department of Biostatistics, University of Pittsburgh, Pittsburgh, PA

and

Lu Tang

Department of Biostatistics, University of Pittsburgh, Pittsburgh, PA

email: lutang@pitt.edu

SUMMARY: Federated learning is an appealing framework for analyzing sensitive data from distributed health data networks. Under this framework, data partners at local sites collaboratively build an analytical model under the orchestration of a coordinating site, while keeping the data decentralized. While integrating information from multiple sources may boost statistical efficiency, existing federated learning methods mainly assume data across sites are homogeneous samples of the global population, failing to properly account for the extra variability across sites in estimation and inference. Drawing on a multi-hospital electronic health records network, we develop an efficient and interpretable tree-based ensemble of personalized treatment effect estimators to join results across hospital sites, while actively modeling for the heterogeneity in data sources through site partitioning. The efficiency of this approach is demonstrated by a study of causal effects of oxygen saturation on hospital mortality and backed up by comprehensive numerical results.

KEY WORDS: Conditional average treatment effect; Data integration; Heterogeneous data sources; Individualized treatment rule; Meta-analysis.

1. Introduction

Data integration approaches have received wide attention in recent years because distributed data networks are becoming commonplace in modern data architecture. A distributed data network allows scalable storage of huge data sets without requiring all data to be physically stored in one central location. Compared to the classic centralized storage scheme, such a distributed data storage framework offers a “cloud” solution to allow more efficient management and maintenance of data in a collaborative environment. Analytically, new statistical and machine learning methods have been proposed to handle such data. They focus on restricting the amount of data exchanged between data sites in order to be communication efficient and to respect the privacy of proprietary data, while suffering a certain loss of statistical efficiency (Chen et al., 2020). Causal modeling, especially personalized treatment effect estimation, could benefit from data integration because the power in every single study is typically very small. With the hope of increasing power and reducing uncertainty, data integration is sought after. However, without properly accounting for the heterogeneity across data sets may introduce more uncertainty, defeating the purpose of data integration.

There are two main types of construct of a distributed database system (Breitbart et al., 1986): homogeneous versus

heterogeneous. In the homogeneous case, data across sites are homogeneous samples of the global population. Data are randomly allocated to each local site, rendering a homogeneous and identically distributed data network. When randomization is not affordable, local data tend to be heterogeneously distributed across the network. We study the latter, a more challenging case when there is too much heterogeneity to warrant direct aggregation of results derived from individual sites. Specifically, we draw our focus on *distributed health data networks* (DHDNs) where sensitive patient-level data are collected and stored locally at individual sites (e.g., hospitals), and propose an analytical framework to harmonize such heterogeneous data, with the goal of improving estimation and prediction. A specific objective is to improve the quantification of *conditional average treatment effect* (CATE) at individual sites by leveraging summarized information shared across a DHDN. DHDNs consist of mainly observational health data where there is no control over how data are distributed. Well-known examples include the Sentinel (Platt et al., 2018) initiative for monitoring product safety and the PCORnet (Fleurence et al., 2014) initiative for clinical research, both are DHDNs that operate on a national scale, among others.

A sensible computing scheme for distributed data is *fed-*

erated learning (Konečný et al., 2016; Yang et al., 2019). Federated learning enlists local sites to collaboratively build an analytical model under the orchestration of a *coordinating site* (i.e., one of the sites designated to communicate with all sites), while keeping patient-level data private and decentralized. Figure 1 illustrates such scheme. Federated learning (i) can easily scale up the total data size by the inclusion of additional sites into the DHDN without sacrificing computational speed, (ii) is appealing for analyzing data from DHDNs that are sensitive in nature, and (iii) bypasses data sharing barriers to encourage site participation in modern-day collaborative research. Its effectiveness has been proven in large-scale epidemiological and clinical research, especially in regression analysis (Li et al., 2019). Most statistical methods proposed for distributed data, including the widely used meta-analysis, fall in this scheme. Despite many federated learning approaches relying on multi-rounds back-and-forth communication that requires full automation, we propose a one-shot approach that requires only one round of communication, because of the non-negligible human effort typically involved.

In the federated learning literature, the homogeneity assumption is commonly adopted. Recent work such as Lee et al. (2017), Battey et al. (2018), Jordan et al. (2019) and Tang et al. (2020) all assume that samples are randomly partitioned, which guarantees equal sample size and identical data distribution across sites. Such an assumption does not hold in most DHDNs. In reality, considerable heterogeneity exists across sites, even in multi-center randomized clinical trials, let alone in observational studies, leading to inconsistently estimated treatment effects. Such heterogeneity could arise if there are unobserved features that reflect the differences in population, treatment quality, infrastructures, among others, resulting in biases in CATE across sites hence poor inference.

Classically, site-level heterogeneity is modeled by a normal random site effect. A random-effects meta-analysis evaluates within-site and between-site heterogeneities (Riley et al., 2011), which are then used to inform the discrepancy between local and global results. There exist non-parametric random-effects modeling approaches such as the cluster-robust causal forest described in Athey and Wager (2019) where the distribution of random effects is not specified. These methods only improve the estimation and generalization of the global treatment effect. However, a global treatment effect is not always warranted when there is a high level of between-site heterogeneity, a commonly seen scenario in practice that renders the global estimate invalid (Borenstein et al., 2011). Random effects only describe site deviation but cannot be used to increase the power of local inference at any specific site, which is in fact a more relevant objective when it comes to precision medicine.

In this paper, we propose a tree-based federated learning approach to model the pattern of heterogeneity in DHDNs, through which to improve estimation and prediction of personalized treatment effects of individual sites. Our approach generalizes federated learning to handle heterogeneously distributed data, which closes the gap between the homogeneous data assumption and real data scenarios that are mostly heterogeneous. The coordinating site in the DHDN does not naively aggregate models from all sites, but assesses the heterogeneity across sites so that only models from sites that

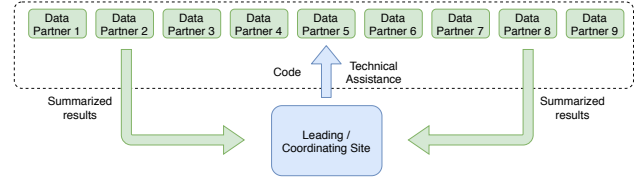


Figure 1: Distributed research network under federated learning framework.

are more similar are aggregated. In essence, we model site-level heterogeneity through site-wise tree splits. Similar sites remain in the same partition hence model information can be shared, yet distinct sites are sorted into different partitions. Site splitting may occur at the subpopulation level, resulting in a flexible information-sharing scheme that is patient characteristic-dependent and site-dependent. For example, the treatment effects in two hospitals may be similar for female patients but different for male patients, requiring us to consider borrowing information across sites only on selective subgroups, i.e., female. The similarity between any two sites is defined based on the CATEs conditioning on subgroups, where the subgroups are defined by covariates. A two-stage procedure is proposed. We first build localized models for the CATE estimation within each site. These localized models are then passed to a coordinating site to assess the heterogeneity across sites based on an augmented data constructed only from data in the coordinating site. A final tree-based model is fit on the augmented data, with treatment effect as the outcome on patient features and site. The conceptual diagram is illustrated in Figure 2 and the rationale is further explained in Section 3.

We organize the paper as follows. A short problem motivation will be given in Section 2 with a brief introduction of the DHDN under consideration. We describe the rationale of the proposed method in detail in Section 3 and estimators for comparison in Section 4. The performance of the proposed method is demonstrated in simulation experiments and a data application in Section 5 and Section 6, respectively. A discussion is provided in Section 7.

2. Data Motivation

Electronic health records (EHR) collected in intensive care units (ICUs) possess a wealth of information on health conditions, treatment, and outcomes of critically ill patients. In ICU patients with cardiorespiratory complications, blood oxygen saturation should be given extra attention. Although low blood oxygen levels are generally considered to be harmful, recent studies have shown that a high level of blood oxygenation could further jeopardize the health of patients (Geoghegan et al., 2018). The British Thoracic Society recommends oxygen therapy at the 94-98% pulse oximetry-derived oxygen saturation (SpO_2) target range (O’driscoll et al., 2017). An earlier retrospective study found that the lowest mortality was observed at a SpO_2 between 94% and 98% among patients requiring oxygen therapy (van den Boom et al., 2020). This study considered a mixed-effects model with a random intercept to mitigate biases due to differences

across hospitals, but failed to account for such biases when optimal treatment rules are drawn. So far, the optimal oxygenation target is still unclear and more studies of oxygen therapy are needed, especially for critically ill ICU patients (Suzuki et al., 2013). Driven by such motivation, we draw on an observational EHR data and a comparable cohort of patients with oxygen therapy from the eICU Collaborative Research Database (eICU-CRD), a multi-hospital database made available by Philips Healthcare (Pollard et al., 2018). Our goal is to investigate the CATE of the oxygen therapy at the SpO₂ 94-98% range on hospital mortality.

Different from earlier works that operated on a large pooled observational cohort, we assume patient-level data from different hospitals cannot be merged, hence the setting where federated learning is required. From a method development perspective, the convenience of using the eICU-CRD data is that data of all sites are accessible, allowing comparison with non-federated learning approaches. Heterogeneity across hospitals is also widely acknowledged (Sheikhalishahi et al., 2020). Unobserved factors could result in differences in hospital infrastructures, healthcare coverage affected by economic levels, or cultural factors such as trust in medical systems (Brookhart et al., 2010), among others, all of which can be related to treatments and outcomes. By viewing hospital sites as a DHDN, our goal is to define “closeness” between hospitals and selectively borrow information from “neighbors” to increase the power of CATE estimation. We hypothesize that the unobserved factors are correlated with sites in a way that we can adjust for potential unobserved factors through site-wise subgrouping. For example, patient comorbidity is typically not available for ICU patients upon admission, yet it is related to hospital types, which is associated with both treatment and outcome, hence should be adjusted for in the CATE estimation. Site-wise partitioning may partially reveal comorbidity differences if patients seek treatments according to their health conditions and corresponding hospital reputation. Hence, it allows us to adjust for such unobserved confounding through subgrouping of sites. Our analysis shows there is strong heterogeneity in treatment effects across sites as compared to the heterogeneity within sites. Section 6 provides the full details of this motivating application.

3. Tree-based Federated Learning

Federated learning can be viewed as constructing a super learner, or a so-called model ensemble, which is more powerful and stable than individual learners (Zhang and Singer, 2010). Existing methods such as bagging, random forest (Breiman, 2001) or boosting (Friedman, 2001) consider learners that are built from randomly sampled data sets, the main goal of which is to reduce variance and improve estimation (Bühlmann and Yu, 2002). We consider a tree-based ensemble that accounts for the between-site heterogeneity when localized learners are built on nonrandomly sampled data. Both trees and forests are considered.

The main objective of the ensemble is to improve personalized treatment effect estimation and prediction within the sites of an existing DHDN. We do not attempt to generalize results beyond the network. It takes locally estimated models obtained at individual sites as input. For personalized

treatment effect estimation, localized models are constructed by estimating CATE functions that are specific to each site. These individually estimated functions are then passed to the coordinating site, say site 1, to estimate an ensemble model that allows information to be shared while appropriately accounting for across-site heterogeneity. The output of the final ensemble is not a unified CATE function, but site-specific CATE functions that can be viewed as improved versions of the individually estimated functions.

The notion of heterogeneity is defined as the similarity between sites. Given two patients with identically observed feature \mathbf{x} but in two different sites, say site A and B, we define the similarity between them based on the target of interest, in this case the CATE functions $\tau_A(\mathbf{x})$ and $\tau_B(\mathbf{x})$. If $\tau_A(\mathbf{x})$ and $\tau_B(\mathbf{x})$ are similar, combining data from the two sites increases the power of estimation. However, because of heterogeneity across sites, $\tau_A(\mathbf{x})$ and $\tau_B(\mathbf{x})$ may be different and cannot be combined. This is different from the similarity based on model coefficients. For example, in a recent approach by Shen et al. (2020), fusion is based on the distance of model parameters. If linear CATE functions $\tau_A(\mathbf{x}) = \mathbf{x}^T \boldsymbol{\beta}_A$ and $\tau_B(\mathbf{x}) = \mathbf{x}^T \boldsymbol{\beta}_B$ are estimated, they define distance based on the confidence distributions of $\boldsymbol{\beta}_A$ and $\boldsymbol{\beta}_B$, which are indirect to the targeted treatment effects. In some cases, $\tau_A(\mathbf{x})$ and $\tau_B(\mathbf{x})$ are nonparametric or built by different models, and we might not have a meaningful comparison of the model coefficients. What further distinguishes our work from earlier work is that we allow the similarity to be varying with \mathbf{x} . Sites can be similar with respect to a subgroup defined by \mathbf{x} but dissimilar elsewhere. Such adaptive distance offers the flexibility to refine the inference targets by selective information borrowing across the network. Before we elaborate on the ensemble construction, we first introduce model assumptions and methods for localized CATE estimation on which the ensemble is based.

3.1 Federated Learning of Personalized Treatment Effects

Let Y denote the outcome of interest, Z denote a binary treatment indicator, and \mathbf{X} denote patient characteristics. Correspondingly, let y , z and \mathbf{x} denote realizations of the random variables. For ease of exposition, we present treatment effects through the potential outcome framework (Neyman, 1923; Rubin, 1974). The classic CATE is defined as the difference in mean of the counterfactual outcomes between two treatment groups for individuals with characteristics \mathbf{X} , that is, $\tau(\mathbf{x}) = E[Y^{(Z=1)} - Y^{(Z=0)} | \mathbf{X} = \mathbf{x}]$, where $Y^{(Z=1)}$ and $Y^{(Z=0)}$ are the counterfactual outcomes under treated $Z = 1$ and control $Z = 0$, respectively. In the case of heterogeneous DHDN, we obtain from site k the CATE function $\tau_k(\mathbf{x}) = E_k[Y^{(Z=1)} - Y^{(Z=0)} | \mathbf{X} = \mathbf{x}]$, where the expectation is taken over the population in that site, for $k = 1, \dots, K$, and K is the total number of sites. We also denote the sample size of site k as n_k , and the total sample size as $N = \sum_{k=1}^K n_k$. Based on a modified unconfoundedness assumption which will be introduced, we have $\tau_k(\mathbf{x}) = E[Y^{(Z=1)} - Y^{(Z=0)} | \mathbf{X} = \mathbf{x}, S = k]$, where we introduce S as the site indicator which can take values $1, \dots, K$. Consider the data setup $\mathcal{D} = \{D_i = [U_i, S_i, \mathbf{X}_i, Z_i, Y_i], i = 1, \dots, N\}$, where for subject i , U_i is the unknown confounding variable, S_i is the study site that the subject comes from, \mathbf{X}_i is the observed feature vector

of the subject, Z_i is the treatment assignment, and Y_i is the observed outcome.

Assumptions. Heterogeneity of treatment effect can be due to unobserved confounding, posing a challenge to the classic assumptions. Given \mathbf{x} , $\tau_k(\mathbf{x})$ obtained from site k may not be the same as $\tau_{k'}(\mathbf{x})$ from another site $k' \neq k$. Thus, for subject i , the standard unconfoundedness assumption $\{Y_i^{(Z=0)}, Y_i^{(Z=1)}\} \perp Z_i | \mathbf{X}_i$ (Rosenbaum and Rubin, 1983) is not sufficient to guarantee estimation consistency. To proceed with heterogeneity across sites, we require the treatment assignment Z_i to be independent of the potential outcomes for Y_i conditional on both \mathbf{X}_i and an unobserved confounder U_i :

$$\{Y_i^{(Z=0)}, Y_i^{(Z=1)}\} \perp Z_i | \mathbf{X}_i, U_i.$$

To allow identifiable treatment effects, we further assume that given site origin S_i , treatment assignment is random and independent of the unobserved U_i that causes heterogeneity:

$$\{Y_i^{(Z=0)}, Y_i^{(Z=1)}, U_i\} \perp Z_i | \mathbf{X}_i, S_i.$$

This means that we can take observations with similar \mathbf{x} among comparable sites from $\{1, \dots, K\}$, and assume that this group comes from a randomized experiment. It also means that site similarity can be used to infer U_i , hence can be used to adjust for unobserved confounding. We refer to this as the modified unconfoundedness assumption for heterogeneous data. In other words, the main source of unobserved heterogeneity is reflected in the differences between sites, not within sites. In addition, we impose the positivity assumptions

$$0 < P(S_i = k | \mathbf{X}_i) < 1, \forall k, \text{ and } 0 < P(Z_i = 1 | \mathbf{X}_i, S_i) < 1,$$

for all \mathbf{X}_i and S_i such that all subjects are possible to be observed in all sites, and all subjects in all sites are possible to receive either arm of treatment.

Localized model: estimation of $\tau_k(\mathbf{x})$ at each site. Estimation of $\tau_k(\mathbf{x})$ at each local site must be obtained separately before the ensemble. Recently published methods on the estimation of individualized treatment effects include causal tree (Athey and Imbens, 2016), causal forest (Wager and Athey, 2018), Bayesian regression tree models (Hahn et al., 2020), deep neural networks (Farrell et al., 2021), among others. On the other hand, meta-learners such as T-learner, S-learner, X-learner (Künzel et al., 2019), and R-learner (Nie and Wager, 2020) that indirectly estimate treatment effects with one or more models of the observed outcome have become increasingly popular. Despite the various choices, we consider the following methods in estimating $\tau_k(\mathbf{x})$ within a given site k : causal tree (CT), causal forest (CF), and X-learner with Bayesian additive regression trees as base learners (XL). They are non-linear learners that enjoy the following convenience: (i) they allow different types of outcome such as discrete and continuous outcome, hence can be applied to a broad range of real data scenarios; (ii) they can easily handle a large number of covariates and high order interactions by construction. A causal forest is a stochastic averaging of multiple causal trees (Athey and Imbens, 2016). In each tree, the mean squared error (MSE) of treatment effect τ is used to select the feature and cutoff point in each split. Causal forest builds deep trees with small leaves

without needing to explicitly estimate the propensity (Wager and Athey, 2018).

X-learner first models outcome functions $E[Y^{Z=1} | \mathbf{X} = \mathbf{x}, S = k]$ and $E[Y^{Z=0} | \mathbf{X} = \mathbf{x}, S = k]$ separately to obtain the CATEs among the treated subjects and among the control subjects with base learners, and then apply propensity-weighting for these two estimates to generate CATE estimate for a new data point \mathbf{x} . We choose Bayesian additive regression trees as base learners as they tend to be robust to hyperparameter tuning and small data sets (Künzel et al., 2019). The causal tree, causal forest, and X-learner are implemented in R packages `causalTree`, `grf`, and `hfe`, respectively.

REMARK 1: Despite our choice of the localized learners in estimating $\tau_k(\mathbf{x})$, the ensemble framework can be applied to any general estimator of $\tau_k(\mathbf{x})$. Similar to a meta-analysis that takes the estimated quantities of interest and their respective variances as input, the proposed method takes estimated functions of interest as input, without pooling patient-level data.

Ensemble of $\{\hat{\tau}_k(\mathbf{x})\}_{k=1}^K$ using site 1 data. The most straightforward way to aggregate multiple estimates is by averaging. An aggregated estimate takes the form $\frac{1}{K} \sum_{k=1}^K \hat{\tau}_k(\mathbf{x})$. It requires all models to be based on random samples of the global study population so that heterogeneity across sites is negligible. Another popular approach is the meta-analysis by combining summary statistics from each site inversely weighted by their respective variances. Different from the above, we consider an ensemble of $\{\hat{\tau}_k(\mathbf{x})\}_{k=1}^K$, which are estimated from a nonoverlapping data partitions that are *not random*. To model heterogeneity, we include a categorical site indicator when building the ensemble so that it can actively adjust for heterogeneity across sites. Since patient-level data cannot be pooled, we construct the ensemble using only data from the coordinating site. Without loss of generality, we designate site 1 for the task. The K estimated models, $\{\hat{\tau}_k(\mathbf{x})\}_{k=1}^K$, are passed to the first site to get K treatment effect estimates for each subject in site 1, resulting in an augmented data:

$$\mathcal{D}_{aug,1} = \{D_{i,k} = [\mathbf{X}_i, k, \hat{\tau}_k(\mathbf{X}_i)], i : S_i = 1, k = 1, \dots, K\}.$$

An ensemble is then trained on this data by either a regression tree or a random forest, with the estimated treatment effects $\hat{\tau}_k(\mathbf{X}_i)$ as the outcome, and a categorical site indicator of which localized model is used along with all patient features as predictors.

In the ensemble, the estimated treatment effect can be represented as $\hat{\tau}(\mathbf{x}, s)$, which depends on both \mathbf{x} and site s . Let $\mathcal{L}(\mathbf{x}, s)$ denote the leaf node corresponding to \mathbf{x} and s . The ensemble tree (ET) estimate based on the augmented site 1 data can be derived by

$$\begin{aligned} \hat{\tau}_{ET}(\mathbf{x}, s) &= \frac{1}{|\{(i, k) : S_i = 1, (\mathbf{X}_i, k) \in \mathcal{L}(\mathbf{x}, s)\}|} \\ &\quad \sum_{\{(i, k) : S_i = 1, (\mathbf{X}_i, k) \in \mathcal{L}(\mathbf{x}, s)\}} \hat{\tau}_k(\mathbf{X}_i) \\ &= \sum_{i=1}^{n_1} \sum_{k=1}^K \frac{\mathbb{1}\{(\mathbf{X}_i, k) \in \mathcal{L}(\mathbf{x}, s)\}}{|\mathcal{L}(\mathbf{x}, s)|} \hat{\tau}_k(\mathbf{X}_i). \end{aligned} \quad (1)$$

This represents the average difference between $Y|Z = 1$ and $Y|Z = 0$ at the leaf node $\mathcal{L}(\mathbf{x}, s)$. Intuitively, observations with similar characteristics (\mathbf{x} and \mathbf{x}') and from similar sites (s and s') are more likely to fall in the same leaf node in the ensemble tree, i.e., $(\mathbf{x}, s) \in \mathcal{L}(\mathbf{x}', s')$ or $(\mathbf{x}', s') \in \mathcal{L}(\mathbf{x}, s)$. This resembles a non-smooth kernel where weights are $1/|\mathcal{L}(\mathbf{x}, s)|$ for observations that are within the neighborhood of (\mathbf{x}, s) , and 0 otherwise. Therefore, our estimator attempts to borrow information from neighbors in the space of \mathbf{X} and S . Due to our assumptions stated above, we can adjust for potential unobserved confounding factor U by adjusting for S through site-wise partitioning. The splits of the tree are based on minimizing in-sample MSE of τ within each leaf and pruning by cross-validation over choices of the complexity parameter. A diagram of the proposed method using a single tree is shown in Figure 2 where site 1 serves as the coordinating site.

Since a single tree is prone to be unstable, we propose a forest version of the ensemble to reduce variance and smooth the partitioning boundaries. An ensemble forest (EF) can be constructed by aggregating many ensemble trees to create soft partitions while still benefit from information sharing across sites. The EF estimate is

$$\begin{aligned}\hat{\tau}_{EF}(\mathbf{x}, s) &= \frac{1}{B} \sum_{b=1}^B \hat{\tau}_b(\mathbf{x}, s) = \sum_{i=1}^{n_1} \sum_{k=1}^K \omega_{i,k}(\mathbf{x}, s) \hat{\tau}_k(\mathbf{X}_i), \\ \omega_{i,k}(\mathbf{x}, s) &= \frac{1}{B} \sum_{b=1}^B \frac{\mathbb{1}\{(\mathbf{X}_i, k) \in \mathcal{L}_b(\mathbf{x}, s)\}}{|\mathcal{L}_b(\mathbf{x}, s)|}\end{aligned}\quad (2)$$

where the form of $\hat{\tau}_b(\mathbf{x}, s)$ closely follows (1) but is based on a subsample of $\mathcal{D}_{aug,1}$. The weights, $\omega_{i,k}(\mathbf{x}, s)$, are similar to that in (1), and can be viewed as kernel weighting that defines an adaptive neighborhood of \mathbf{x} and s . Each site can contribute partial information but not all or none. If we fix s at $s = 1$, $\tau_{EF}(\mathbf{x}, s = 1)$ is viewed as a re-estimation of the original $\tau_1(\mathbf{x})$ but with information from other sites incorporated. As our simulations in Section 5 show, this improves the original estimator $\tau_1(\mathbf{x})$ that is based on site 1 only. The total number of trees in a forest is set at $B = 2000$ throughout the paper. Tree and forest estimates can be obtained by R packages `rpart` and `ranger`, respectively. Once the federated model is obtained, we may broadcast it back to local sites for validation, prediction, and deployment. We provide an algorithmic overview of the proposed federated learning strategy with ensemble forest in Algorithm 1. Our method has been implemented in the R package `ifedtree` available on Github (github.com/ellenxtan/ifedtree, see Web Appendix C).

REMARK 2: With focus on just a single site, say site s , the proposed ensemble estimators $\hat{\tau}_{ET}(\mathbf{x}, s)$ and $\hat{\tau}_{EF}(\mathbf{x}, s)$ can be regarded as improved versions of the local estimator $\hat{\tau}_s(\mathbf{x})$ through leveraging information from other sites. How much of information being shared is dependent on the ensemble tree construct, with a hard neighborhood assignment in a tree where two sites are either neighbors or not neighbors, and a soft neighborhood assignment in a forest. Note that the neighborhood is dependent on \mathbf{x} .

3.2 Federated Learning with Different Goals

The proposed approach applies not only to the conditional average treatment effect function $\tau_k(\mathbf{x})$, but to any general

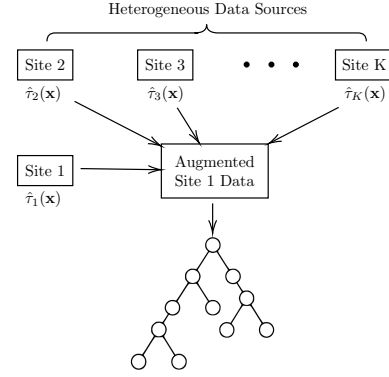


Figure 2: Schema of the proposed algorithm. Functions of the estimated treatment effects from K local sites are first generated independently. They are then passed into a coordinating site (say site 1) to get K predicted treatment effects for each subject in site 1, resulting in a new augmented site 1 data. With the augmented site 1 data, a federated model can be trained by either a regression tree (as shown) or a random forest, with the estimated treatment effects as the outcome. A site indicator of which localized model is used along with the patient characteristics is fed into the federated model as covariates. Once the federated model is obtained, we may broadcast it back to local sites for deployment.

Algorithm 1 Tree-based federated learning for heterogeneous data sources

- 1: **for** $k \leftarrow 1, 2, \dots$ to K **do** \triangleright Loop through K sites. Can be run in parallel.
 - 2: Build a localized model using site k data.
 - 3: **end for**
 - 4: **for** $i \leftarrow 1, 2, \dots$ to n_1 **do** \triangleright Loop through n_1 subjects in site 1.
 - 5: **for** $k \leftarrow 1, 2, \dots$ to K **do** \triangleright Loop through K localized models.
 - 6: Predict $\hat{\tau}_k(\mathbf{x}_i)$ for subject i in site 1 using localized model k .
 - 7: $D_{i,k} \leftarrow [\mathbf{x}_i, k, \hat{\tau}_k(\mathbf{x}_i)]$.
 - 8: **end for**
 - 9: **end for**
 - 10: Create augmented site 1 data $\mathcal{D}_{aug,1}$ by concatenating $D_{i,k}$ vectors.
 - 11: $\hat{\tau}_{EF}(\mathbf{x}, s) \leftarrow \text{ENSEMBLEFOREST}(\mathcal{D}_{aug,1})$ \triangleright Or `ENSEMBLETREE`.
-

function $f_k(\mathbf{x})$ of interest. We put our focus on the CATE due to the ubiquitous pooling of heterogeneous data in studies of precision medicine. Typically, studies are powered only for average treatment effects. Thus, estimation and inference for CATE suffer from loss of power because of sample attrition due to conditioning (Assmann et al., 2000). This type of question can nicely leverage the benefit of data integration.

Most federated learning approaches focus on the inference for the global population, where the sites are considered random. We argue that this is ambitious for treatment effect estimation, especially when data are heterogeneous. For example, in the random-effects meta-analysis, standard practice

is to report the prediction intervals of the global effect alongside its confidence intervals. Prediction intervals are used to generalize results beyond existing sites. But they are usually much wider than confidence intervals and are hard to interpret in practice. As a result, modeling sites as a random effect provides limited use in precision medicine as compared to just treating sites as fixed (i.e., site-specific treatment effects). Random effects estimation also becomes numerically unstable when the number of sites associated with the random effect is small, resulting in convergence issues.

We treat sites as fixed and focuses on improving the estimation and prediction of CATE within the given sites of a DHDN, which may be more crucial to answering the need for personalized medicine. Other approaches along this line consider integrating likelihood functions (Tang and Song, 2016), estimating equations (Tang and Song, 2020), and decision models (Qiu, 2018, Chapter 4). However, they require pooling of patient-level data.

4. Estimators for Heterogeneous Data Sources

Within the tree-based federated learning framework introduced in Section 3, we develop two versions of estimators using *adaptive* and *honest* estimation (Athey and Imbens, 2016), depending on whether separate training data are used for tree building and tree estimation. Adaptive approaches use the same training data for both model selection (in our case, building partitions of the feature space) as well as estimation based on a model structure. This approach could lead to biases because the selected model could be affected by potential spurious correlations between covariates and outcomes. Fortunately, as the sample size grows, biases disappear and give rise to a small estimation error. Alternatively, honest approaches separate the training sample into two halves, one half for building the tree model, and another half for estimating treatment effects within the leaves. Although the honest version enjoys unbiased estimation, it may suffer from low precision as it only uses part of the training sample in the estimation phase. Section 3.1 develops our estimators for the ensemble regression tree and the ensemble regression forest model. Depending on whether CT, CF, or XL is used to construct localized models and whether ET or EF is used to construct the ensemble, we denote the corresponding estimator as {CT, CF, XL}-{ET, EF}.

Several other methods are considered for comparison. A baseline approach for federated learning is aggregation. Treatment effect estimates from sites are directly averaged to form the final estimates, which is $\hat{\tau}_{agg}(\mathbf{x}) = \frac{1}{K} \sum_{k=1}^K \hat{\tau}_k(\mathbf{x})$, where $\hat{\tau}_k(\mathbf{x})$ is the local estimates from site k . We denote the aggregated estimator based on the different localized models as {CT, CF, XL}-agg. Another alternative method is based on a random-effects meta-analysis model where site-specific variations in $\tau(\mathbf{x})$, i.e., $u_{k,\mathbf{x}} = \tau_k(\mathbf{x}) - \tau(\mathbf{x})$, $k = 1, \dots, K$, are considered random following a normal distribution, $u_{1,\mathbf{x}}, \dots, u_{K,\mathbf{x}} \sim N(0, \sigma^2(\mathbf{x}))$, at a given \mathbf{x} . Localized models from sites are passed to site 1 to get treatment effect estimates and the corresponding standard errors from all models for the site 1 subjects. Those estimates are then combined by a random-effects meta-analysis with site being

random. We denote the meta-analysis estimator based on the different localized models as {CT, CF, XL}-meta.

In contrast to federated learning approaches that assume patient-level data cannot be shared across sites, we also consider the hypothetical analysis when centralized data are available, taking advantage of simulated data. Following Athey and Wager (2019), we build a centralized model using the cluster-robust causal forest for comparison. This is a non-parametric random-effects model and is flexible in that we do not need to specify the distribution of random site effects. Different from the random forest that directly draws subsamples of observations, cluster-robust causal forest first draws a subsample of clusters and then draws a subsample of observations randomly from each cluster. We denote this centralized approach as clustCF and it could be implemented with the R package `grf`.

A high-level summary of the properties of the proposed federated estimator and other estimators is provided in Table 1. The proposed methods possess the most desired features.

5. Simulation Study

Monte Carlo simulations are conducted to assess the proposed methods. We assume there are $K = 20$ sites in total, each with a sample size $n = 100$. We specify $m(\mathbf{x}, k)$ as the conditional mean of outcome and $\tau(\mathbf{x}, k)$ as the conditional treatment effect for individuals in site k . The marginal treatment probability is $P = 0.5$. The potential outcomes can be written as

$$Y_i(z) = m(\mathbf{X}_i, S_i) + \frac{1}{2} \cdot (2z - 1) \cdot \tau(\mathbf{X}_i, S_i) + \epsilon_i,$$

where $z = 0, 1$, and $\epsilon_i \sim N(0, 1)$. Denote the number of features as D . Features \mathbf{X}_i are assumed to be independent of ϵ_i , and $\mathbf{X}_i \sim N(\mathbf{0}, \mathbf{I})$. Assuming two underlying groups among the K sites ($\mathcal{G}_1 = \{k : k \bmod 2 = 1\} = \{1, 3, \dots, K-1\}$; $\mathcal{G}_2 = \{k : k \bmod 2 = 0\} = \{2, 4, \dots, K\}$), we simulate data from the following designs under a heterogeneous DHDN.

- (1) Null design: $D = 3$; $m(\mathbf{x}, k) = 0$;
 $\tau(\mathbf{x}, k) = -4 \cdot \mathbb{1}\{k \in \mathcal{G}_2\}$.
- (2) Complex non-linear design: $D = 4$; $m(\mathbf{x}, k) = 0$;
 $\tau(\mathbf{x}, k) = \varsigma(x_1)\varsigma(x_2) - 4 \cdot \mathbb{1}\{k \in \mathcal{G}_2\} + x_1 \cdot \mathbb{1}\{k \in \mathcal{G}_2\}$,
 $\varsigma(x) = \frac{2}{1+e^{-12(x-1/2)}}$.
- (3) Simple piece-wise linear design: $D = 5$;
 $m(\mathbf{x}, k) = \frac{1}{2}x_1 + \sum_{d=2}^4 x_d - 4 \cdot \mathbb{1}\{k \in \mathcal{G}_2\} + x_1 \cdot \mathbb{1}\{k \in \mathcal{G}_2\}$;
 $\tau(\mathbf{x}, k) = \mathbb{1}\{x_1 > 0\} \cdot x_1 - 4 \cdot \mathbb{1}\{k \in \mathcal{G}_2\} + x_1 \cdot \mathbb{1}\{k \in \mathcal{G}_2\}$.
- (4) Complex piece-wise linear design: $D = 8$;
 $m(\mathbf{x}, k) = \frac{1}{2} \sum_{d=1}^2 x_d + \sum_{d=3}^6 x_d - 4 \cdot \mathbb{1}\{k \in \mathcal{G}_2\} + x_1 \cdot \mathbb{1}\{k \in \mathcal{G}_2\}$;
 $\tau(\mathbf{x}, k) = \sum_{d=1}^2 \mathbb{1}\{x_d > 0\} \cdot x_d - 4 \cdot \mathbb{1}\{k \in \mathcal{G}_2\} + x_1 \cdot \mathbb{1}\{k \in \mathcal{G}_2\}$.

The designs within sites are similar to those in Athey and Imbens (2016), Wager and Athey (2018), and Künzel et al. (2019). Covariates in $\tau(\mathbf{x}, k)$ are predictive markers while covariates in $m(\mathbf{x}, k)$ but not in $\tau(\mathbf{x}, k)$ are prognostic only. Design 1 represents the situation when none of the covariates are predictive of treatment effects. We consider complex linear and non-linear scenarios in designs 2, 3, and 4 where sites from the same underlying groupings have similar treatment effects

Table 1: Comparison of characteristics of our proposed federated models with other methods on analyzing heterogeneous data sources.

	Not require pooling data from all sites	Borrow information from other sites	Consider heterogeneity across sites	Reveal heterogeneity site patterns	Focus on each individual site
Proposed federated models	✓	✓	✓	✓	✓
Local modelling only	✓	×	×	×	✓
Clustered-robust causal forest	×	✓	✓	×	×
Random-effects meta-analysis	✓	✓	✓	✓	×
Mean aggregation	✓	✓	×	×	×

and mean effects, while sites from different underlying groupings have different treatment effects and mean effects. Odd sites and even sites form two distinct groups. Correspondingly, we consider these designs under a homogeneous DHDN where site populations are random samples of the global population.

- (1) Null design: $D = 3$; $m(\mathbf{x}, k) = 0$; $\tau(\mathbf{x}, k) = 0$.
- (2) Complex non-linear design: $D = 4$; $m(\mathbf{x}, k) = 0$;
 $\tau(\mathbf{x}, k) = \varsigma(x_1)\varsigma(x_2)$, $\varsigma(x) = \frac{2}{1+e^{-12(x-1/2)}}$.
- (3) Simple piece-wise linear design: $D = 5$;
 $m(\mathbf{x}, k) = \frac{1}{2}x_1 + \sum_{d=2}^4 x_d$;
 $\tau(\mathbf{x}, k) = \mathbb{1}\{x_1 > 0\} \cdot x_1$.
- (4) Complex piece-wise linear design: $D = 8$;
 $m(\mathbf{x}, k) = \frac{1}{2} \sum_{d=1}^2 x_d + \sum_{d=3}^6 x_d$;
 $\tau(\mathbf{x}, k) = \sum_{d=1}^2 \mathbb{1}\{x_d > 0\} \cdot x_d$.

We compare the proposed methods with several other methods in the performance of predicting treatment effects of an independent test data generated from site 1 (the coordinating site). Methods being compared include localized models, and other federated and non-federated learning methods discussed in Section 4. Specifically, we report the empirical bias and MSE over an independent test samples of sample size n from site 1 where $\text{Bias}(\hat{\tau}) = \frac{1}{n} \sum_{i=1}^n \{\hat{\tau}(\mathbf{x}_i, k=1) - \tau(\mathbf{x}_i, k=1)\}$; $\text{MSE}(\hat{\tau}) = \frac{1}{n} \sum_{i=1}^n \{\hat{\tau}(\mathbf{x}_i, k=1) - \tau(\mathbf{x}_i, k=1)\}^2$.

Among the three localized models {CT, CF, XL}, XL has the best performance in all designs. Hence, in Table 2, we compare the performance of different data integration methods with XL as the local learner. Results of the proposed methods (XL-ET, XL-EF) from adaptive estimation are presented. The proposed methods, especially XL-EF, achieve the lowest MSEs in nearly all designs under both heterogeneous and homogeneous data networks, outperforming the aggregation approach (XL-agg), meta-analysis (XL-meta), and even the centralized robust approach (clustCF). Comparing ET to EF, EF has an even smaller bias and MSE, which is expected because forest models tend to be more stable and accurate than tree models as a result of aggregation. Note that for all designs under the homogeneous data network, the centralized approach clustCF achieves minimal bias and MSE compared to other methods. This is expected as clustCF takes advantage of individual-level data from all sites. For designs 1 and 2 under the homogeneous designs, meta-analysis achieves comparable performance as our proposed methods. However, it fails to achieve desirable results in the heterogeneous data network. In terms of bias, our proposed federated estimators tend to have larger biases compared to the localized model XL, although

Table 2: Simulation results comparing multiple methods with X-learner as the localized model.

Design	Model	Heterogeneous sites		Homogeneous sites	
		Bias $\times 100$	MSE	Bias $\times 100$	MSE
1	XL	0.047	1.7×10^{-3}	0.047	1.7×10^{-3}
	XL-EF	-0.012	3.0×10^{-4}	-6.9×10^{-3}	3.3×10^{-4}
	XL-ET	-0.035	8.7×10^{-6}	0.129	1.0×10^{-3}
	XL-meta	-200.042	4.009	-0.041	4.8×10^{-4}
	XL-agg	-199.755	3.990	0.245	7.2×10^{-6}
	clustCF	-199.800	4.094	0.032	1.1×10^{-3}
2	XL	-0.253	0.542	-0.253	0.542
	XL-EF	-6.630	0.482	-8.020	0.487
	XL-ET	-13.046	0.806	-13.788	0.501
	XL-meta	-207.864	4.875	-13.070	0.461
	XL-agg	-201.947	5.189	-5.731	1.118
	clustCF	-199.400	4.332	-4.0×10^{-3}	6.2×10^{-3}
3	XL	1.646	0.191	1.646	0.191
	XL-EF	2.638	0.098	8.480	0.097
	XL-ET	19.655	0.214	12.457	0.131
	XL-meta	-170.744	3.080	22.916	0.168
	XL-agg	-175.174	3.405	21.408	0.385
	clustCF	-199.900	4.813	0.131	0.019
4	XL	0.369	0.395	0.369	0.395
	XL-EF	6.713	0.252	6.956	0.262
	XL-ET	8.286	0.395	6.699	0.323
	XL-meta	-168.396	3.324	8.572	0.299
	XL-agg	-172.917	3.668	18.306	0.718
	clustCF	-200.500	4.815	-0.145	0.072

their biases are much smaller compared to meta-analysis and the aggregation approach. By borrowing information from additional sites, variances are greatly reduced, resulting in a small MSE of the federated estimators. We provide results of the honest version of XL-ET and XL-EF in Web Table 1. Honest estimation tends to have comparatively larger MSEs due to training sample splitting but smaller biases. We defer results of using CT and CF as localized models and their corresponding federated models to Web Table 2 and Web Table 3, respectively, to show the robustness of the proposed methods. The local models of choice are rather competitive estimators. A comparison with $n = 500$ is provided in Web Table 4 to show that the proposed methods tend to provide more improvement to a local model alone when n is small.

Figure 3 visualizes the results of design 2 under heterogeneous data network using adaptive XL-ET and XL-EF method, respectively. Figure 3a plots the learned ensemble tree. Site is used as a splitting rule at the root node, and recovers the underlying grouping of the true model. Features

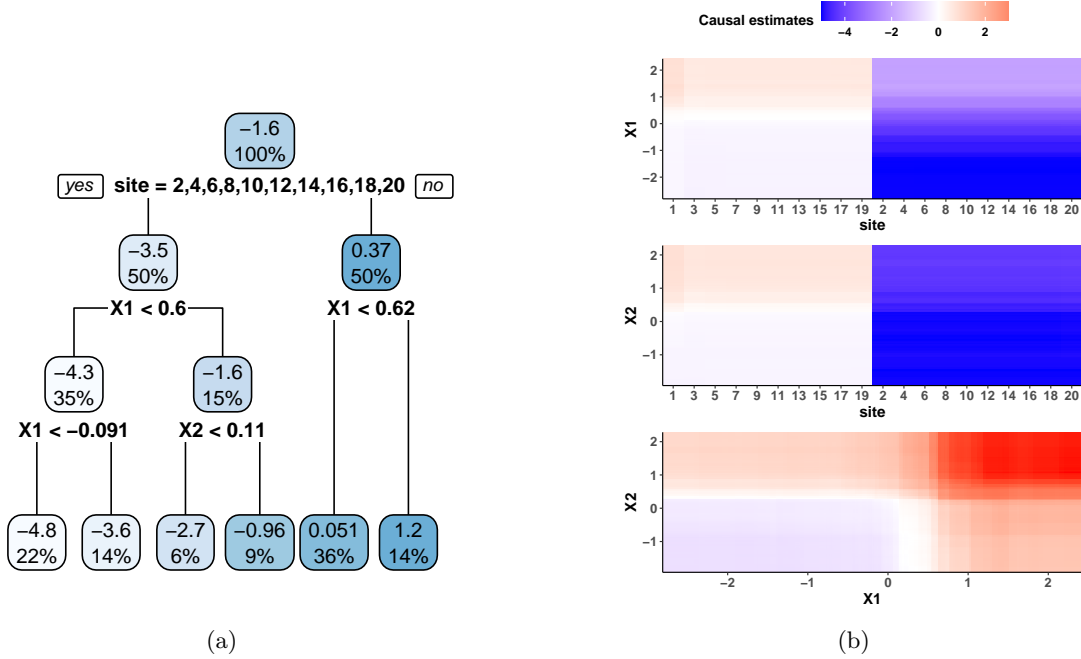


Figure 3: Visualization of design 2 under heterogeneous data network using XL-ET (a) and XL-EF (b). (a) Each node shows the estimated treatment effects and the percentage of observations in the node. Under each internal node is the corresponding splitting rule. In the tree, the site indicator is the root node, recovering the fact that odd sites and even sites form two distinct groups. X_1 and X_2 are other variables appearing on the tree, which is consistent as they are the only two covariates involved in simulating the $\tau(\mathbf{x}, k)$. (b) Estimation of causal effects for different values of X_1 in each site, different values of X_2 in each site, and different values of X_1 and X_2 , respectively. The odd sites are arranged first, followed by the even sites. The plot recovers the underlying groupings across sites and the heterogeneity between subjects within site 1 is also consistent with the ground truth.

X_1 and X_2 are selected, which is consistent with the fact that X_1 and X_2 are the only two important features for $\tau(\mathbf{x}, k)$ in design 2. Figure 3b shows the treatment effect estimates in the ensemble forest for different values of X_1 in each site, different values of X_2 in each site, and different values of X_1 and X_2 , respectively. The color of each grid is the estimated average causal estimates among subjects with a certain value of the covariate of interest in a certain site, with values of other covariates fixed at their expected value. The model is able to recover the underlying groupings across sites indicated by the distinct colors for odd sites and even sites. There is also treatment effect heterogeneity between subjects within each site as indicated by the color gradients of grids within sites, which is consistent with the ensemble tree results and the ground truth. EF is preferred in practice because it yields a more accurate and stable estimation.

6. Data Application: eICU-CRD Distributed Hospital EHR Data Network

As introduced in Section 2, we provide a detailed analysis on the causal effects of oxygen saturation SpO_2 within the range of 94% to 98% on hospital mortality among critically ill patients with respiratory diseases and with at least 48-hour of oxygen therapy. From the eICU-CRD multi-hospital electronic health records network, a total of 12,626 ICU

patients from 127 sites are obtained. We consider SpO_2 within the range of 94% to 98% as the treatment arm and SpO_2 outside of the range as the control arm. The final analysis cohort consists of 7,022 patients from 20 hospitals, each with at least 50 patients on each treatment arm. Hospital-level information for the 20 hospitals is provided in Web Table 5. We use the same covariates as in van den Boom et al. (2020), which are age, body mass index (BMI), sex, Sequential Organ Failure Assessment (SOFA) score, and duration of oxygen therapy. Adaptive XL-EF is applied, with hospital 1 being the coordinating site.

Figure 4a plots the ensemble forest estimation of treatment effects for different values of covariates in each site, respectively, with subfigures ranked by the relative importance of the covariates. Strong between-site heterogeneity and some within-site heterogeneity are indicated by the different color gradients of the grids between and within sites. Relative feature importance shown in Figure 4b is measured by the total decrease in node impurity defined by MSE that results from splits over a feature, averaged over all trees, scaled by the sum of importance across all features. In the generated forest, heterogeneity across sites dominates that of patient characteristics. For better interpretation, the best linear projection (Semenova and Chernozhukov, 2017) of the estimated treatment effects of the coordinating site from XL-EF is mapped into the patient characteristics space. The coefficients from the doubly robust linear model fit are -0.002, -0.001, 0.0002,

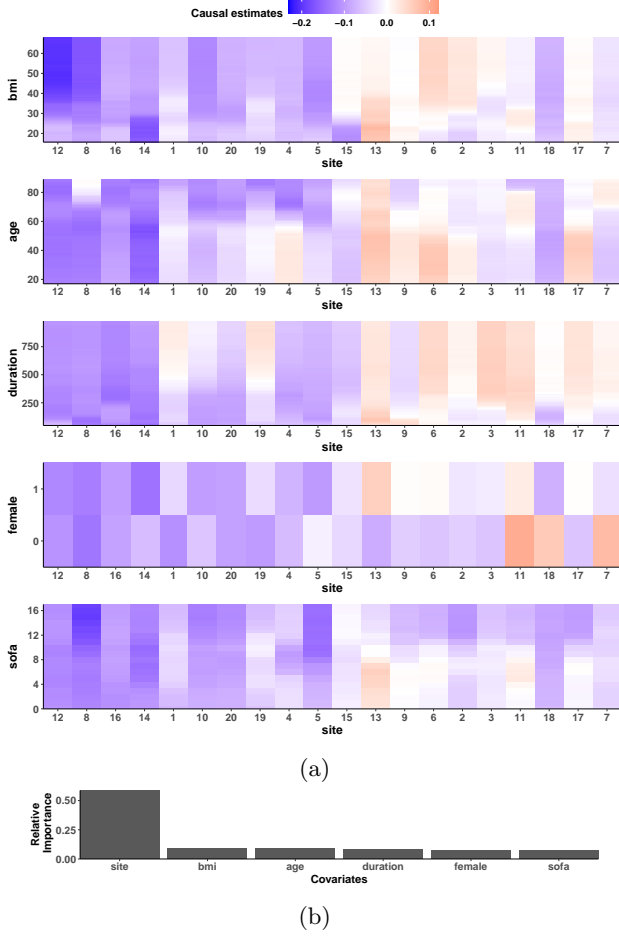


Figure 4: Visualization of treatment effects estimation of oxygen saturation on hospital mortality with site 1 as the coordinating site using XL-EF method. (a) Estimation of causal effects for different values of covariates in each site, respectively. The interpretation of is similar to that in Figure 3b. There are apparent within-site heterogeneity and across-site heterogeneity indicated by the different color gradients of the grids within and across sites. (b) Variable importance plot in the ensemble forest. The site indicator is the most important variable in the ensemble forest, with importance taking up 58.8%.

0.13, 0.016 for BMI, age, oxygen therapy duration, gender, and SOFA score, respectively, with none of these covariates significant under the significance level of 0.05. These results indicate strong between-site heterogeneity in treatment effect in comparison to within-site heterogeneity.

Hospitals in the South and are non-teaching hospitals tend to have larger negative causal effects. However, as there is limited hospital information, further research is needed to investigate the site-level heterogeneity. In this application, different hospitals have different sample sizes n_k . Those with a smaller sample size may not be representative of the population, leading to an uneven level of precision for local causal estimates $\tau_k(\mathbf{x})$. To account for different sample sizes at each hospital, we consider a basic weighting strategy where we add weights to $\hat{\tau}_k(\mathbf{x})$ in the EF adjusting for the sample size of

site k . The weights are defined as $w_k(\mathbf{x}) = Kn_k / \sum_{j=1}^K n_j$. Results show similar patterns as in Figure 4 as well as similar coefficients of the best linear projection of mapping the estimated CATEs to patient characteristic space. The detailed results of this weighting strategy are provided in Web Appendix B. Sensitivity to the choice of coordinating site is also assessed by choosing other sites as the coordinating site. Similar results are obtained as those in Figure 4, assuring that the ensemble is robust over the choice of coordinating site. The detailed results of the sensitivity analysis are provided in Web Appendix B. In practice, each site can take turns to serve as the coordinating site, which reduces the influence of using one specific site as the coordinating site, as suggested in Duan et al. (2021).

Overall, the results show evidence that there are moderate causal effects of oxygen saturation being in the range of 94% to 98% on hospital mortality. However, the causal effects could vary across sites. This could provide insights for identifying the optimal range of SpO_2 that could help to reduce hospital mortality in clinical practice.

7. Discussion

In this paper, we have proposed an efficient and interpretable tree-based ensemble framework for personalized treatment effect estimation in the setting of distributed data where patient-level data cannot be pooled. Such kind of data scheme is increasingly common in practice and we hope to highlight the importance of accounting for data heterogeneity through this work. We break the traditional thinking of viewing data integration as being a yes or no decision. Instead, the proposed approaches explore the similarity and dissimilarity of the targeted treatment effect between sites to yield an optimal information-sharing scheme for selectively improving the treatment effect of interest.

Throughout the paper, we focus on the problems of estimation and prediction of the conditional average treatment effects. The construction of confidence intervals for conditional treatment effects in the ensemble model remains challenging due to the extra uncertainty from the localized estimates. Our experience using the infinitesimal jackknife for random forests (Wager et al., 2014; Wager and Athey, 2018) shows that the federated estimators fail to achieve satisfactory performance in terms of nominal coverage of a confidence interval. Nevertheless, by borrowing information from multiple sites, variances are greatly reduced, resulting in a small MSE in terms of the final estimated treatment effect. Sites in the distributed data networks may have uneven sample sizes, as we have demonstrated in our data application. Improvements to the weighting strategy are needed to allow considering the treatment proportion as well as covariate distributions across sites in order to further improve the federated estimator.

We also stress that despite the function of interest in this paper being the conditional treatment effect, a more general $f(\mathbf{x})$ still applies and may be of interest to other research problems where data are heterogeneous. For example, in a longitudinal study of outcome-time association $y = f(t)$ where there is a large amount of between-individual heterogeneity, in which case individuals will be treated as sites, or in a meta-

analysis of genome-wide association studies where auxiliary patient-level data from one of the sites are available.

SUPPORTING INFORMATION

Web Appendices referenced in Sections 5, 6, and R code of the proposed methods may be found online in the Supporting Information.

REFERENCES

- Assmann, S. F., Pocock, S. J., Enos, L. E., and Kasten, L. E. (2000). Subgroup analysis and other (mis) uses of baseline data in clinical trials. *The Lancet* **355**, 1064–1069.
- Athey, S. and Imbens, G. (2016). Recursive partitioning for heterogeneous causal effects. *Proceedings of the National Academy of Sciences* **113**, 7353–7360.
- Athey, S. and Wager, S. (2019). Estimating treatment effects with causal forests: An application. *arXiv preprint arXiv:1902.07409*.
- Battey, H., Fan, J., Liu, H., Lu, J., and Zhu, Z. (2018). Distributed testing and estimation under sparse high dimensional models. *Annals of Statistics* **46**, 1352–1382.
- Borenstein, M., Hedges, L. V., Higgins, J. P., and Rothstein, H. R. (2011). *Introduction to meta-analysis*. John Wiley & Sons.
- Breiman, L. (2001). Random forests. *Machine Learning* **45**, 5–32.
- Breitbart, Y., Olson, P. L., and Thompson, G. R. (1986). Database integration in a distributed heterogeneous database system. In *1986 IEEE Second International Conference on Data Engineering*, pages 301–310. IEEE.
- Brookhart, M. A., Stürmer, T., Glynn, R. J., Rassen, J., and Schneeweiss, S. (2010). Confounding control in healthcare database research: challenges and potential approaches. *Medical Care* **48**, S114–S120.
- Bühlmann, P. and Yu, B. (2002). Analyzing bagging. *The Annals of Statistics* **30**, 927–961.
- Chen, D.-G., Liu, D., Min, X., and Zhang, H. (2020). Relative efficiency of using summary versus individual data in random-effects meta-analysis. *Biometrics*.
- Duan, R., Ning, Y., and Chen, Y. (2021). Heterogeneity-aware and communication-efficient distributed statistical inference. *Biometrika* asab007.
- Farrell, M. H., Liang, T., and Misra, S. (2021). Deep neural networks for estimation and inference. *Econometrica* **89**, 181–213.
- Fleurence, R. L., Curtis, L. H., Califf, R. M., Platt, R., Selby, J. V., and Brown, J. S. (2014). Launching PCORnet, a national patient-centered clinical research network. *Journal of the American Medical Informatics Association* **21**, 578–582.
- Friedman, J. H. (2001). Greedy function approximation: a gradient boosting machine. *Annals of Statistics* **28**, 1189–1232.
- Geoghegan, P., Keane, S., and Martin-Loeches, I. (2018). Change is in the air: dying to breathe oxygen in acute respiratory distress syndrome? *Journal of Thoracic Disease* **10**, S2133.
- Hahn, P. R., Murray, J. S., Carvalho, C. M., et al. (2020). Bayesian regression tree models for causal inference: Regularization, confounding, and heterogeneous effects (with discussion). *Bayesian Analysis* **15**, 965–1056.
- Jordan, M. I., Lee, J. D., and Yang, Y. (2019). Communication-efficient distributed statistical inference. *Journal of the American Statistical Association* **114**, 668–681.
- Konečný, J., McMahan, H. B., Yu, F. X., Richtárik, P., Suresh, A. T., and Bacon, D. (2016). Federated learning: strategies for improving communication efficiency. *arXiv preprint arXiv:1610.05492*.
- Künzel, S. R., Sekhon, J. S., Bickel, P. J., and Yu, B. (2019). Metalearners for estimating heterogeneous treatment effects using machine learning. *Proceedings of the National Academy of Sciences* **116**, 4156–4165.
- Lee, J. D., Liu, Q., Sun, Y., and Taylor, J. E. (2017). Communication-efficient sparse regression. *The Journal of Machine Learning Research* **18**, 115–144.
- Li, X., Fireman, B. H., Curtis, J. R., Arterburn, D. E., Fisher, D. P., Moyneur, É., Gallagher, M., Raebel, M. A., Nowell, W. B., Lagreid, L., and Toh, S. (2019). Validity of privacy-protecting analytical methods that use only aggregate-level information to conduct multivariable-adjusted analysis in distributed data networks. *American Journal of Epidemiology* **188**, 709–723.
- Neyman, J. (1923). Sur les applications de la thar des probabilités aux expériences agricoles: Essay des principe. Excerpts reprinted (1990) in English. *Statistical Science* **5**, 463–472.
- Nie, X. and Wager, S. (2020). Quasi-oracle estimation of heterogeneous treatment effects. *arXiv preprint arXiv:1712.04912*.
- O’driscoll, B., Howard, L., Earis, J., and Mak, V. (2017). BTS guideline for oxygen use in adults in healthcare and emergency settings. *Thorax* **72**, ii1–ii90.
- Platt, R., Brown, J. S., Robb, M., McClellan, M., Ball, R., Nguyen, M. D., and Sherman, R. E. (2018). The FDA sentinel initiative—an evolving national resource. *New England Journal of Medicine* **379**, 2091–2093.
- Pollard, T. J., Johnson, A. E., Raffa, J. D., Celi, L. A., Mark, R. G., and Badawi, O. (2018). The eICU collaborative research database, a freely available multi-center database for critical care research. *Scientific Data* **5**, 180178.
- Qiu, X. (2018). *Statistical Learning Methods for Personalized Medicine*. PhD thesis, Columbia University.
- Riley, R. D., Higgins, J. P., and Deeks, J. J. (2011). Interpretation of random effects meta-analyses. *BMJ* **342**.
- Rosenbaum, P. R. and Rubin, D. B. (1983). The central role of the propensity score in observational studies for causal effects. *Biometrika* **70**, 41–55.
- Rubin, D. B. (1974). Estimating causal effects of treatments in randomized and nonrandomized studies. *Journal of Educational Psychology* **66**, 688.
- Semenova, V. and Chernozhukov, V. (2017). Debiased machine learning of conditional average treatment effects and other causal functions. *arXiv preprint arXiv:1702.06240*.

- Sheikhalishahi, S., Balaraman, V., and Osmani, V. (2020). Benchmarking machine learning models on multi-centre eicu critical care dataset. *PloS ONE* **15**, e0235424.
- Shen, J., Liu, R. Y., and Xie, M.-g. (2020). i fusion: Individualized fusion learning. *Journal of the American Statistical Association* **115**, 1251–1267.
- Suzuki, S., Eastwood, G. M., Peck, L., Glassford, N. J., and Bellomo, R. (2013). Current oxygen management in mechanically ventilated patients: a prospective observational cohort study. *Journal of Critical Care* **28**, 647–654.
- Tang, L. and Song, P. X. (2016). Fused lasso approach in regression coefficients clustering: learning parameter heterogeneity in data integration. *The Journal of Machine Learning Research* **17**, 3915–3937.
- Tang, L. and Song, P. X.-K. (2020). Poststratification fusion learning in longitudinal data analysis. *Biometrics*.
- Tang, L., Zhou, L., and Song, P. X.-K. (2020). Distributed simultaneous inference in generalized linear models via confidence distribution. *Journal of Multivariate Analysis* **176**, 104567.
- van den Boom, W., Hoy, M., Sankaran, J., Liu, M., Chahed, H., Feng, M., and See, K. C. (2020). The search for optimal oxygen saturation targets in critically ill patients: observational data from large icu databases. *Chest* **157**, 566–573.
- Wager, S. and Athey, S. (2018). Estimation and inference of heterogeneous treatment effects using random forests. *Journal of the American Statistical Association* **113**, 1228–1242.
- Wager, S., Hastie, T., and Efron, B. (2014). Confidence intervals for random forests: The jackknife and the infinitesimal jackknife. *The Journal of Machine Learning Research* **15**, 1625–1651.
- Yang, Q., Liu, Y., Chen, T., and Tong, Y. (2019). Federated machine learning: concept and applications. *ACM Transactions on Intelligent Systems and Technology* **10**, 1–19.
- Zhang, H. and Singer, B. H. (2010). *Recursive Partitioning and Applications*. Springer Science & Business Media.

**“A Tree-based Federated Learning Approach for Personalized Treatment Effect
Estimation from Heterogeneous Data Sources”**

by Xiaoqing Tan, Chung-Chou H. Chang and Lu Tang

Web Appendix A. Full Simulation Results

We provide full simulation results for using XL, CT, CF as local models in this section. The number of replications is 500 throughout. Two versions of our proposed federated methods, *adaptive* estimation and *honest* estimation respectively with regards to sample splitting as in Athey and Imbens (2016) and (Wager and Athey, 2018), are presented. The results of methods with XL, CT, CF as the localized model are presented in Web Table 1, Web Table 2, and Web Table 3, respectively. We use (A) to denote the adaptive version and (H) to denote the honest version wherever applicable. Overall, the results of the honest version are similar to that of the adaptive version. The honest approaches tend to achieve a smaller bias while the adaptive versions enjoy a relatively small MSE. Our proposed federated estimators, especially the ensemble forest (EF) exhibits a satisfactory performance compared to the meta-analysis, mean aggregation, and cluster-robust causal forest under the heterogeneous data network. Under the homogeneous network, clustCF shows a very competitive performance, as it takes advantage of individual-level data from all sites. Our proposed estimators are robust under the homogeneous sites. We compare results of $n = 500$ for localized models and the proposed federated models with XL as the localized model in Web Table 4.

[Table 1 about here.]

[Table 2 about here.]

[Table 3 about here.]

[Table 4 about here.]

Web Appendix B. Additional Results for Data Application

In real-life applications, various hospitals may have sample sizes n_k . Web Table 5 shows hospital-level information for the 20 hospitals where the number of patients across sites varies. Information includes the region of the U.S. where the hospital is located, whether it is a teaching hospital, the bed capacity, and the number of patients within the hospital.

Hospitals with a smaller sample size may not be representative of the population, leading to an uneven level of precision for local causal estimates $\tau_k(\mathbf{x})$. To account for different sample sizes at each hospital, we consider a basic weighting strategy where we add weights to $\hat{\tau}_k(\mathbf{x})$ in the EF adjusting for the sample of site k . The weights are defined as

$$w_k(\mathbf{x}) = \frac{Kn_k}{\sum_{j=1}^K n_j}.$$

Web Figure 1 visualizes the estimation of treatment effects for different values of covariates in each site, respectively, with subfigures ranked by the relative importance of the covariates. Similar patterns as Figure 4 are shown as there is strong between-site heterogeneity followed by some within-site heterogeneity indicated by the different color gradients of the grids between and within sites. For the best linear projection (Semenova and Chernozhukov, 2017) of the estimated treatment effects of the coordinating site from XL-EF, the estimated coefficients from the doubly robust linear model fit are very similar to the results without weighting, which are -0.002, -0.001, 0.0002, 0.13, 0.016 for BMI, age, oxygen therapy duration, gender, and SOFA score, respectively, with none of these covariates significant under the significance level of 0.05. These results strengthen the conclusion that there is strong between-site heterogeneity while the within-site heterogeneity is marginal. For sensitivity analysis, we show heterogeneity pattern of using site 2 and site 3 as the coordinating site, respectively in Web Figure 2 and Web Figure 3. The patterns of within-site heterogeneity and across-site heterogeneity are similar to Figure 4, which indicates the robustness of our proposed estimators.

[Table 5 about here.]

[Figure 1 about here.]

[Figure 2 about here.]

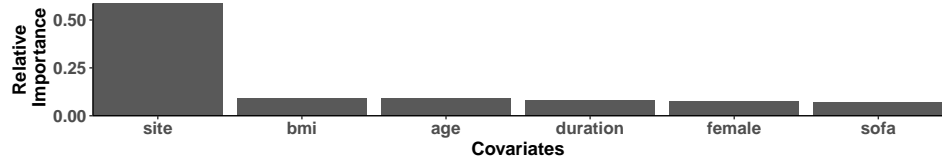
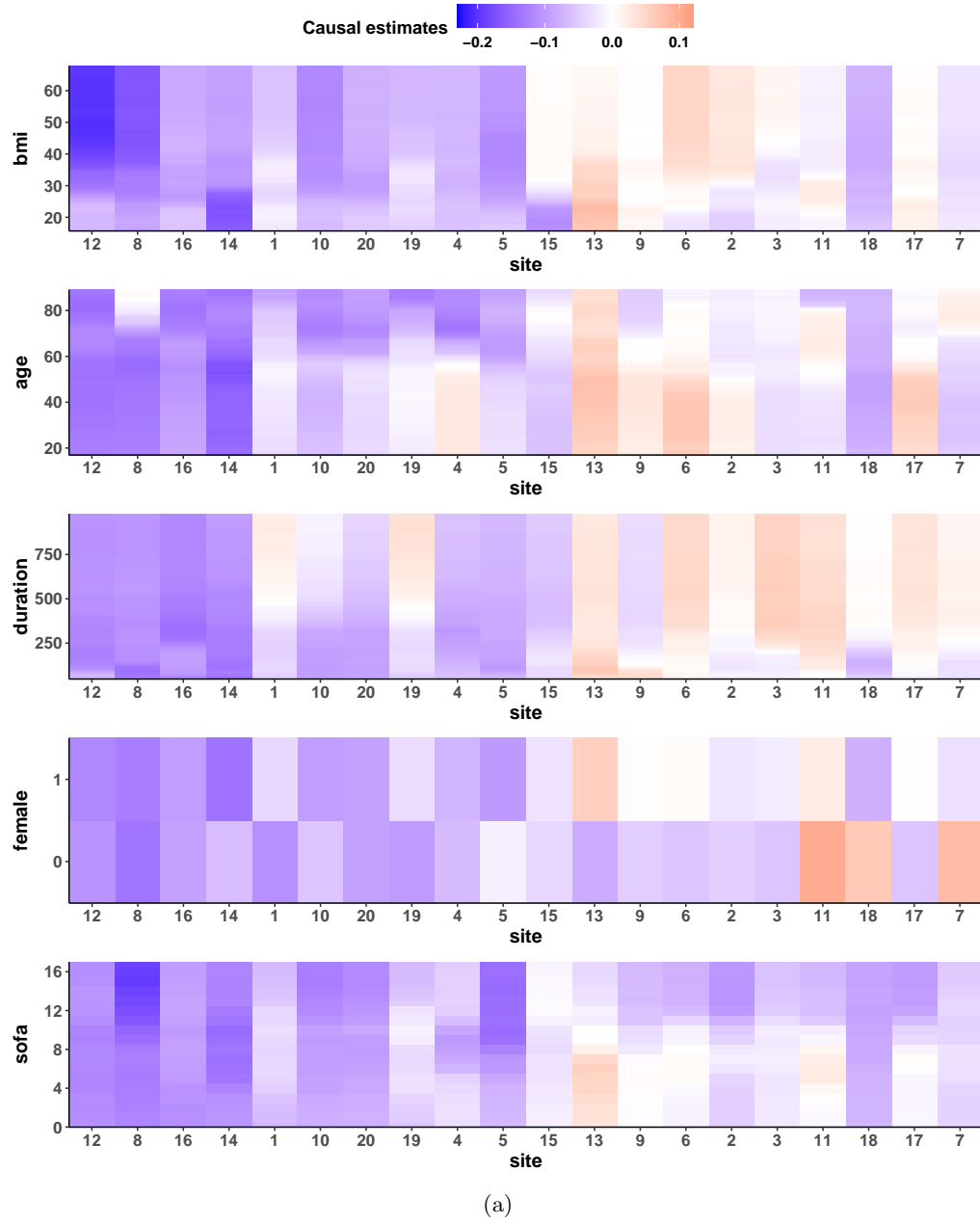
[Figure 3 about here.]

Web Appendix C. R Package and Replication Code

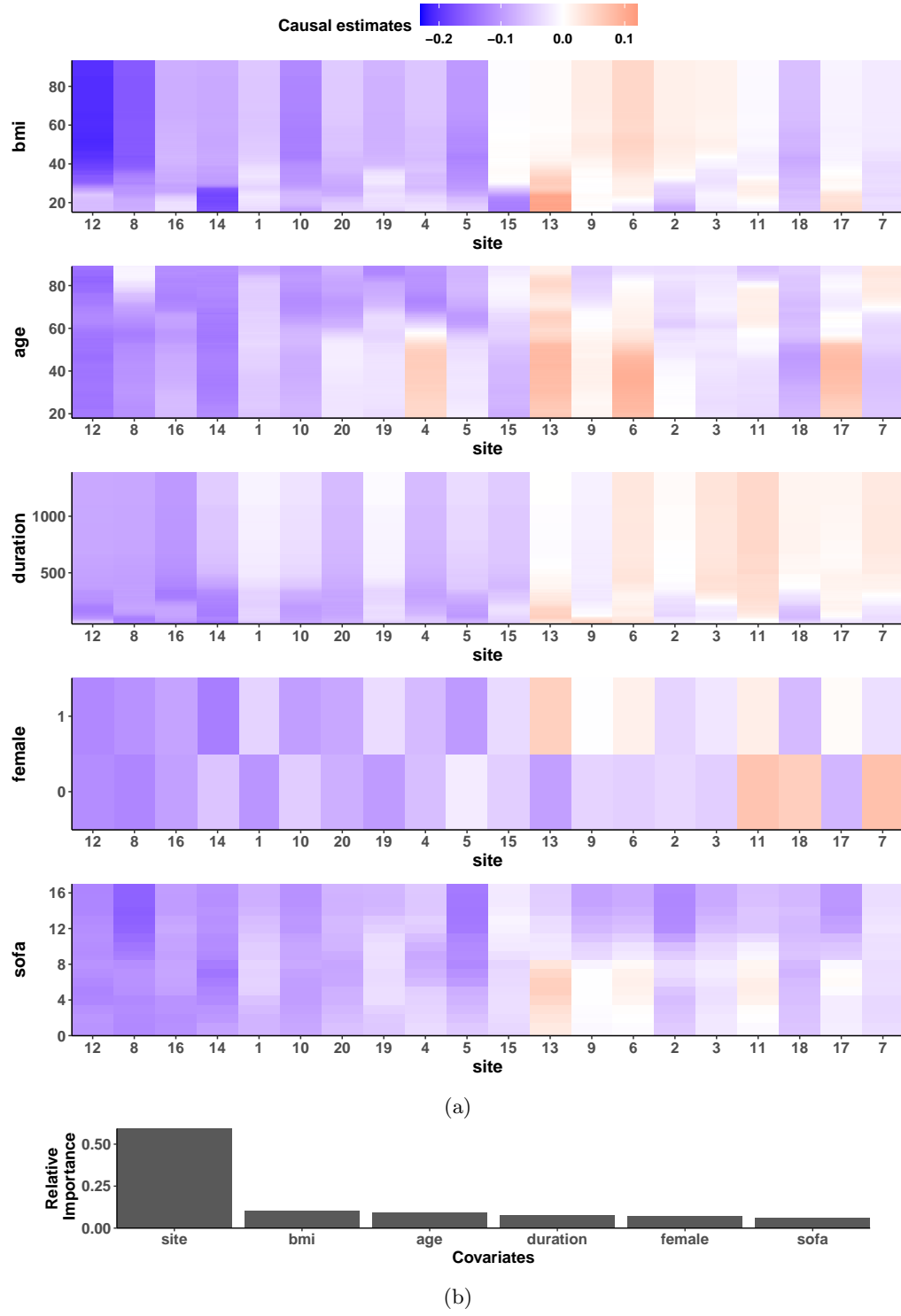
The proposed method has been implemented in the R package `ifedtree` and has been made available on Github (github.com/ellenxtan/ifedtree). Although the eICU-CRD data used in our application example cannot be shared subject to data use agreement, access can be individually requested at <https://eicu-crd.mit.edu/gettingstarted/access/>. We also provide on Github the R code used to replicate the simulation and data application results presented in the paper.

References

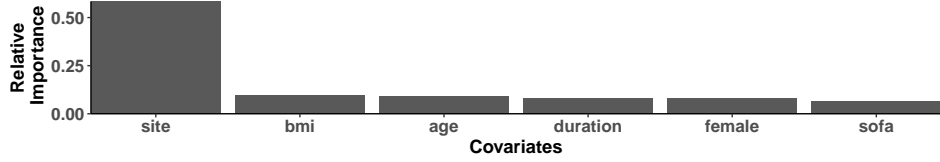
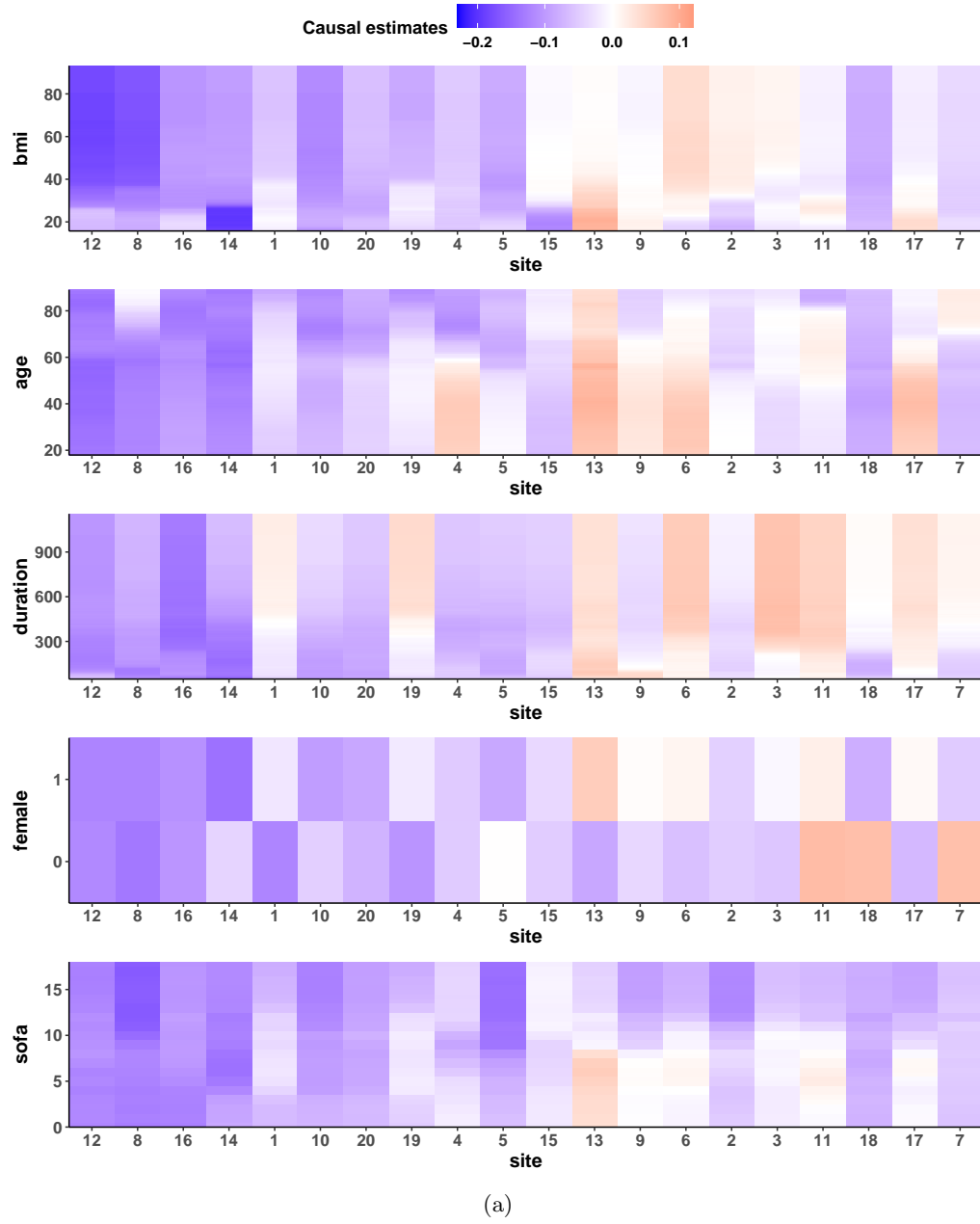
- Athey, S. and Imbens, G. (2016). Recursive partitioning for heterogeneous causal effects. *Proceedings of the National Academy of Sciences* **113**, 7353–7360.
- Semenova, V. and Chernozhukov, V. (2017). Debiased machine learning of conditional average treatment effects and other causal functions. *arXiv preprint arXiv:1702.06240*.
- Wager, S. and Athey, S. (2018). Estimation and inference of heterogeneous treatment effects using random forests. *Journal of the American Statistical Association* **113**, 1228–1242.



Web Figure 1: Visualization of causal effects estimation of oxygen saturation on hospital mortality with site 1 as the coordinating site and a site sample size weighting strategy using XL-EF method. (a) Estimation of causal effects for different values of covariates in each site, respectively. The heterogeneity patterns are similar to Figure 4. (b) Variable importance plot in the ensemble forest. The site indicator is the most important variable in the ensemble forest, with importance taking up 58.7%.



Web Figure 2: Visualization of causal effects estimation of oxygen saturation on hospital mortality with site 2 as the coordinating site using XL-EF method. (a) Estimation of causal effects for different values of covariates in each site, respectively. The pattern of within-site heterogeneity and across-site heterogeneity are similar to Figure 4. (b) Variable importance plot in the ensemble forest. The site indicator is the most important variable in the ensemble forest, with importance taking up 59.2%.



Web Figure 3: Visualization of causal effects estimation of oxygen saturation on hospital mortality with site 3 as the coordinating site using XL-EF method. (a) Estimation of causal effects for different values of covariates in each site, respectively. The pattern of within-site heterogeneity and across-site heterogeneity are similar to Figure 4. (b) Variable importance plot in the ensemble forest. The site indicator is the most important variable in the ensemble forest, with importance taking up 58.3%.

Web Table 1: Simulation results comparing multiple methods with X-learner (XL) as the localized model. The sample size at each site is $n = 100$. “(A)” denotes adaptive version and “(H)” denotes honest version if applicable.

Design	Model	Heterogeneous sites		Homogeneous sites	
		Bias $\times 100$	MSE	Bias $\times 100$	MSE
1	XL	0.047	1.7×10^{-3}	0.047	1.7×10^{-3}
	XL-EF (A)	-0.012	3.0×10^{-4}	-6.9×10^{-3}	3.3×10^{-4}
	XL-EF (H)	-0.050	2.6×10^{-4}	-3.3×10^{-3}	3.1×10^{-4}
	XL-ET (A)	-0.035	8.7×10^{-6}	0.129	1.0×10^{-3}
	XL-ET (H)	-0.036	9.5×10^{-6}	0.184	8.3×10^{-4}
	XL-meta	-200.042	4.009	-0.041	4.8×10^{-4}
	XL-agg	-199.756	3.990	0.245	7.2×10^{-6}
	clustCF (A)	-199.800	4.094	0.032	1.1×10^{-3}
	clustCF (H)	-200.000	4.010	0.036	1.4×10^{-4}
2	XL	-0.253	0.542	-0.253	0.542
	XL-EF (A)	-6.630	0.482	-8.020	0.487
	XL-EF (H)	-7.744	0.485	-8.811	0.489
	XL-ET (A)	-13.046	0.806	-13.788	0.501
	XL-ET (H)	-12.836	0.804	-13.706	0.502
	XL-meta	-207.864	4.875	-13.070	0.461
	XL-agg	-201.947	5.189	-5.731	1.118
	clustCF (A)	-199.400	4.332	-4.0×10^{-3}	6.2×10^{-3}
	clustCF (H)	-199.900	4.192	0.051	0.012
3	XL	1.646	0.191	1.646	0.191
	XL-EF (A)	2.638	0.098	8.480	0.097
	XL-EF (H)	5.558	0.084	11.100	0.093
	XL-ET (A)	19.655	0.214	12.457	0.131
	XL-ET (H)	19.675	0.226	13.678	0.126
	XL-meta	-170.744	3.080	22.916	0.168
	XL-agg	-175.174	3.405	21.408	0.385
	clustCF (A)	-199.900	4.813	0.131	0.019
	clustCF (H)	-200.301	4.205	0.147	0.011
4	XL	0.369	0.395	0.369	0.395
	XL-EF (A)	6.713	0.252	6.956	0.262
	XL-EF (H)	7.267	0.237	7.038	0.249
	XL-ET (A)	8.286	0.395	6.699	0.323
	XL-ET (H)	8.117	0.404	8.115	0.319
	XL-meta	-168.396	3.324	8.572	0.299
	XL-agg	-172.917	3.668	18.306	0.718
	clustCF (A)	-200.500	4.815	-0.145	0.072
	clustCF (H)	-200.200	4.257	0.232	0.067

Web Table 2: Simulation results comparing multiple methods with causal tree (CT) as the localized model. The sample size at each site is $n = 100$. “(A)” denotes adaptive version and “(H)” denotes honest version if applicable.

Design	Model	Heterogeneous sites		Homogeneous sites	
		Bias $\times 100$	MSE	Bias $\times 100$	MSE
1	CT	0.215	3.5×10^{-3}	0.215	3.5×10^{-3}
	CT-EF (A)	-0.381	2.7×10^{-4}	8.0×10^{-3}	7.4×10^{-5}
	CT-EF (H)	-0.235	1.9×10^{-4}	8.9×10^{-3}	7.4×10^{-5}
	CT-ET (A)	0.017	8.9×10^{-5}	0.248	2.1×10^{-3}
	CT-ET (H)	0.011	9.3×10^{-5}	0.219	1.7×10^{-3}
	CT-meta	-200.202	4.010	0.012	1.5×10^{-4}
	CT-agg	-199.983	4.000	0.015	4.3×10^{-5}
	clustCF (A)	-199.800	4.094	0.032	1.1×10^{-3}
	clustCF (H)	-200.001	4.009	0.036	1.4×10^{-4}
2	CT	0.384	0.971	0.384	0.971
	CT-EF (A)	-0.863	0.817	0.182	0.800
	CT-EF (H)	-0.421	0.848	0.211	0.821
	CT-ET (A)	-1.225	1.065	0.629	0.914
	CT-ET (H)	-1.262	1.064	0.459	0.903
	CT-meta	-200.947	4.763	-0.545	0.743
	CT-agg	-200.838	5.158	-1.503	1.124
	clustCF (A)	-199.400	4.332	-4.0×10^{-3}	6.2×10^{-3}
	clustCF (H)	-199.900	4.192	0.051	0.012
3	CT	-5.204	1.224	-5.204	1.224
	CT-EF (A)	-3.801	0.456	-2.546	0.436
	CT-EF (H)	-3.125	0.471	-2.545	0.449
	CT-ET (A)	-1.773	0.547	-4.422	0.780
	CT-ET (H)	-2.609	0.546	-3.796	0.679
	CT-meta	-201.212	4.203	-0.454	0.239
	CT-agg	-199.712	4.345	-0.083	0.352
	clustCF (A)	-199.900	4.813	0.131	0.012
	clustCF (H)	-200.300	4.205	0.147	0.011
4	CT	2.776	1.902	2.776	1.902
	CT-EF (A)	1.744	0.885	3.958	0.856
	CT-EF (H)	2.444	0.913	3.741	0.887
	CT-ET (A)	0.987	1.021	2.389	1.331
	CT-ET (H)	-0.129	0.958	2.949	1.221
	CT-meta	-200.606	4.508	-0.203	0.563
	CT-agg	-199.260	4.670	0.712	0.696
	clustCF (A)	-200.500	4.815	-0.145	0.072
	clustCF (H)	-200.201	4.257	0.232	0.067

Web Table 3: Simulation results comparing multiple methods with causal forest (CF) as the localized model. The sample size at each site is $n = 100$. “(A)” denotes adaptive version and “(H)” denotes honest version if applicable.

Design	Model	Heterogeneous sites		Homogeneous sites	
		Bias $\times 100$	MSE	Bias $\times 100$	MSE
1	CF	0.133	4.7×10^{-4}	0.133	4.7×10^{-4}
	CF-EF (A)	-0.135	6.0×10^{-5}	0.025	1.9×10^{-5}
	CF-EF (H)	-0.105	5.3×10^{-5}	0.024	1.9×10^{-5}
	CF-ET (A)	0.039	4.2×10^{-5}	0.119	4.2×10^{-4}
	CF-ET (H)	0.039	4.3×10^{-5}	0.141	4.2×10^{-4}
	CF-meta	-200.058	4.000	0.021	2.2×10^{-5}
	CF-agg	-200.059	4.000	0.025	1.8×10^{-5}
	clustCF (A)	-199.800	4.094	0.032	1.1×10^{-3}
	clustCF (H)	-200.000	4.009	0.036	1.4×10^{-4}
2	CF	0.301	0.947	0.301	0.947
	CF-EF (A)	0.265	0.968	0.834	0.959
	CF-EF (H)	0.888	0.968	0.845	0.963
	CF-ET (A)	-0.138	1.124	0.060	0.981
	CF-ET (H)	-0.145	1.124	0.029	0.981
	CF-meta	-199.388	4.842	-2.875	0.949
	CF-agg	-200.271	5.135	-0.258	1.123
	clustCF (A)	-199.400	4.332	-4.0×10^{-3}	6.2×10^{-3}
	clustCF (H)	-199.900	4.192	0.051	0.012
3	CF	-0.580	0.316	-0.580	0.316
	CF-EF (A)	-1.584	0.305	-0.095	0.304
	CF-EF (H)	-0.471	0.309	-0.051	0.305
	CF-ET (A)	0.425	0.344	-0.795	0.324
	CF-ET (H)	0.449	0.344	-0.645	0.323
	CF-meta	-198.032	4.106	0.097	0.279
	CF-agg	-200.309	4.356	0.418	0.342
	clustCF (A)	-199.900	4.813	0.131	0.019
	clustCF (H)	-200.300	4.205	0.147	0.011
4	CF	0.541	0.685	0.541	0.685
	CF-EF (A)	-0.142	0.658	1.089	0.658
	CF-EF (H)	0.578	0.675	1.108	0.669
	CF-ET (A)	-0.243	0.699	0.453	0.725
	CF-ET (H)	0.0771	0.699	0.460	0.724
	CF-meta	-197.884	4.450	-0.042	0.611
	CF-agg	-200.460	4.704	0.174	0.684
	clustCF (A)	-200.500	4.815	-0.145	0.072
	clustCF (H)	-200.200	4.257	0.232	0.067

Web Table 4: Simulation results comparing localized model and federated model with X-learner (XL) as the localized model. The sample size at each site is $n = 500$. “(A)” denotes adaptive version and “(H)” denotes honest version if applicable.

Design	Model	Heterogeneous settings		Homogeneous settings	
		Bias $\times 100$	MSE	Bias $\times 100$	MSE
1	XL	-0.120	8.03×10^{-4}	-0.120	8.03×10^{-4}
	XL-EF (A)	0.581	8.08×10^{-4}	0.616	9.10×10^{-4}
	XL-EF (H)	0.585	7.81×10^{-4}	0.619	9.04×10^{-4}
	XL-ET (A)	0.596	3.82×10^{-5}	0.417	6.49×10^{-4}
	XL-ET (H)	0.589	3.80×10^{-5}	0.407	6.61×10^{-4}
2	XL	-0.165	0.016	-0.165	0.016
	XL-EF (A)	1.763	0.021	1.807	0.023
	XL-EF (H)	1.738	0.020	1.838	0.023
	XL-ET (A)	-1.055	0.125	-0.436	0.049
	XL-ET (H)	-0.894	0.124	-0.463	0.047
3	XL	-0.251	0.028	-0.251	0.028
	XL-EF (A)	-0.913	0.012	-0.996	0.014
	XL-EF (H)	-0.918	0.011	-0.991	0.013
	XL-ET (A)	-1.286	0.088	-1.362	0.019
	XL-ET (H)	-1.229	0.088	-1.374	0.019
4	XL	-0.195	0.058	-0.195	0.058
	XL-EF (A)	0.635	0.033	0.618	0.036
	XL-EF (H)	0.601	0.031	0.615	0.034
	XL-ET (A)	-0.335	0.251	-0.670	0.083
	XL-ET (H)	-0.303	0.252	-0.545	0.084

Web Table 5: Hospital-level information of our analysis cohort in eICU-CRD database.

Hospital site	Number of patients	Number of control	Number of treated	Bed capacity	Teaching status	Region
1	477	205	272	≥ 500	False	South
2	388	94	294	≥ 500	False	Midwest
3	464	129	335	≥ 500	True	South
4	523	162	361	≥ 500	False	South
5	149	71	78	250 - 499	False	South
6	305	174	131	≥ 500	False	South
7	297	109	188	≥ 500	True	West
8	210	78	132	Unknown	False	Unknown
9	183	52	131	250 - 499	False	West
10	379	161	218	≥ 500	True	Midwest
11	659	165	494	≥ 500	True	Midwest
12	200	55	145	250 - 499	False	South
13	166	64	102	100 - 249	False	Midwest
14	222	58	164	250 - 499	False	South
15	163	58	105	≥ 500	True	Midwest
16	747	185	562	≥ 500	True	Northeast
17	435	240	195	≥ 500	True	South
18	234	70	164	≥ 500	True	Midwest
19	474	229	245	≥ 500	False	South
20	347	109	238	≥ 500	True	Midwest